Cancer Cell
Article

Expression of Autotaxin and Lysophosphatidic Acid Receptors Increases Mammary Tumorigenesis, Invasion, and Metastases

Shuying Liu,[1] Makiko Umezu-Goto,[1] Mandi Murph,[1] Yiling Lu,[1] Wenbin Liu,[2] Fan Zhang,[1] Shuangxing Yu,[1] L. Clifton Stephens,[3] Xiaojiang Cui,[5,6] George Murrow,[7] Kevin Coombes,[2] William Muller,[8] Mien-Chie Hung,[4] Charles M. Perou,[7] Adrian V. Lee,[5] Xianjun Fang,[9] and Gordon B. Mills[1,*]
[1]Department of Systems Biology
[2]Department of Bioinformatics and Computational Biology
[3]Department of Veterinary Medicine and Surgery
[4]Department of Molecular and Cellular Oncology
University of Texas M.D. Anderson Cancer Center, Houston, TX 77030, USA
[5]Lester and Sue Smith Breast Center, Baylor College of Medicine, Houston, TX 77030, USA
[6]Department of Molecular Oncology, John Wayne Cancer Institute Saint John's Health Center, Santa Monica, CA 90404, USA
[7]Lineberger Comprehensive Cancer Center, University of North Carolina at Chapel Hill, Chapel Hill, NC 27599, USA
[8]McGill Cancer Centre, Montreal, Quebec, H3G 1Y6, Canada
[9]Department of Biochemistry and Molecular Biology, Virginia Commonwealth University, Richmond, VA 23298, USA
*Correspondence: gmills@mdanderson.org
DOI 10.1016/j.ccr.2009.03.027

SUMMARY

Lysophosphatidic acid (LPA) acts through high-affinity G protein-coupled receptors to mediate a plethora of physiological and pathological activities associated with tumorigenesis. LPA receptors and autotaxin (ATX/LysoPLD), the primary enzyme producing LPA, are aberrantly expressed in multiple cancer lineages. However, the role of ATX and LPA receptors in the initiation and progression of breast cancer has not been evaluated. We demonstrate that expression of ATX or each *edg* family LPA receptor in mammary epithelium of transgenic mice is sufficient to induce a high frequency of late-onset, estrogen receptor (ER)-positive, invasive, and metastatic mammary cancer. Thus, ATX and LPA receptors can contribute to the initiation and progression of breast cancer.

INTRODUCTION

Breast cancer remains the most frequent malignant tumor among North American women (Jemal et al., 2007). Standard treatment modalities have improved the overall outlook and quality of life. However, additional targeted therapeutics are needed because of the heterogeneity of breast cancer and primary or acquired resistance to existing therapies. Transgenic mouse models of human breast cancer have provided important information related to the initiation and progression of breast cancer and have emerged as powerful tools for preclinical research. LPA is a bioactive phospholipid that acts as a growth factor by activating distinct high-affinity G protein-coupled receptors (GPCRs) to elicit multiple cellular responses, including proliferation, survival, motility, invasion, and production of growth factors and, in particular, neovascularizing factors (Van Corven et al., 1989; Moolenaar et al., 2004). The endothelial differentiation gene (*edg*) GPCR subfamily (*lpa1/edg2*, *lpa2/edg4*, and *lpa3/edg7*) represents the most widely expressed and well-characterized LPA receptors. ATX, a secreted enzyme, mediates the production of the majority of extracellular LPA by hydrolyzing lysophosphatidylcholine, the most abundant

SIGNIFICANCE

We demonstrate that ATX and LPA receptors play a causal role in breast tumorigenesis by generating transgenic, MMTV-LTR-driven, wild-type human LPA receptor or ATX mice. Mammary cancers occur in the absence of other oncogenic stresses, in a mammary cancer-resistant strain, FVB/N, and are frequently estrogen receptor (ER) positive, invasive, and metastatic—characteristics of human breast cancers that are rarely recapitulated in murine models. Thus, ATX and LPA receptors can contribute to breast cancer initiation and progression. Since ATX and LPA receptor inhibitors are in preclinical development, this work highlights LPA receptors and ATX as potential therapeutic targets that could improve the outcome for breast cancer patients.

lysophospholipid constituent in circulation (Umezu-Goto et al., 2002). Indeed, mice with heterozygous loss of ATX have approximately half the normal plasma levels of LPA (Van Meeteren et al., 2006). Although ATX can produce sphingosine 1 phosphate in vitro, its activity in vivo appears to be restricted to production of LPA (Van Meeteren et al., 2006; Pamuklar et al., 2009).

LPA was initially implicated in cancer pathophysiology by our demonstration that LPA is present at elevated levels in ascites of patients with ovarian cancer and activates ovarian and breast cancer cells (Xu et al., 1995). Subsequent studies have implicated LPA and its receptors in multiple functions in cancer cells, including breast cancer lines (Sasagawa et al., 1999; Fang et al., 2000; Shida et al., 2003; Umezu-Goto et al., 2004; Boucharaba et al., 2004, 2006; Kitayama et al., 2004; Chen et al., 2007; Horak et al., 2007). LPA protects breast cancer cells from the effects of radiation and chemotherapy, suggesting that it could alter response to therapy in patients (Hu et al., 2005; Ishdorj et al., 2008). The LPA1 receptor contributes to the metastasis of breast cancer xenografts to bone (Boucharaba et al., 2004, 2006). Furthermore, LPA1 and the Nm23 metastases regulator are inversely correlated in breast cancer tissues, implicating LPA1 in metastases (Horak et al., 2007). LPA2 is markedly elevated in the majority of postmenopausal breast cancers (Kitayama et al., 2004). Even though these studies suggest a potential contribution of LPA and its receptors in breast tumorigenesis, the role of LPA receptors and/or ATX in initiation, progression, metastases, and outcome of breast cancer remains to be fully elucidated. Furthermore, since LPA signals through GPCRs, which are targets of almost one-half of all drugs (Schlyer and Horuk, 2006), and since LPA receptor and ATX inhibitors are in preclinical development (Baker et al., 2006; Murph and Mills, 2007; www.lpath.com), demonstration that ATX or LPA receptors contribute to breast cancer initiation or progression would increase the impetus for a concerted evaluation of LPA receptor and ATX antagonists as therapeutic interventions. Evaluating the role of ATX and LPA receptors in breast cancer pathophysiology, as well as translating these concepts to effective patient therapy, is hindered, in part, by a lack of suitable animal models.

In this study, we established transgenic mouse models expressing human ATX, the enzyme producing LPA, and each of the three major LPA receptors (LPA1, LPA2, and LPA3) under the MMTV-LTR promoter. Strikingly, the expression of ATX or LPA1, LPA2, or LPA3 was sufficient to result in a high frequency of late-onset mammary carcinomas with variable incidence and metastatic rates.

RESULTS

ATX and LPA Receptor Levels in Breast Cancer Correlate with Clinical Characteristics

As indicated by microarray analysis (Finak et al., 2008), ATX, LPA1, LPA2, and LPA3 are expressed in both human breast epithelium and stroma (see Figure S1A available online). Although LPA1 levels appeared lower in human breast epithelium, there were no statistically significant differences in levels in ATX, LPA1, LPA2, and LPA3 between stroma and epithelium. In normal mammary glands of wild-type (WT) FVB/N mice, LPA1, LPA3, and ATX were expressed at significant levels (Figure S2). LPA2 was low to absent in the mammary gland. According to expression profiling of human breast cancers, ATX, LPA1, LPA2, and LPA3 are expressed in most tumors, with levels of LPA2 and LPA3 being increased in poorly differentiated breast cancers (Sotiriou et al., 2006; Desmedt et al., 2007; Figure S1B; data not shown). Thus, LPA receptor expression could contribute to patient outcomes.

Generation and Characterization of MMTV-*lpa* and MMTV-*atx* Transgenic Mice

To determine whether ATX or *edg* family LPA receptors could play a role in initiation or progression during mammary tumorigenesis, we generated transgenic mice with WT, full-length human *atx*, or FLAG epitope-tagged (because of the lack of useful isoform specific antibodies) *lpa1*, *lpa2*, or *lpa3* cDNA under the control of the MMTV-LTR promoter (Figure 1A; Ngan et al., 2002). Integration of the construct into the genome of FVB/N potential founders was screened by PCR and confirmed by Southern blotting of tail DNA (Figure 1B). Three MMTV-*lpa1* (#LPA1-2, #LPA1-7, and #LPA1-27) and two MMTV-*lpa2* (#LPA2-3 and #LPA2-6), MMTV-*lpa3* (#LPA3-3 and #LPA3-22) and MMTV-*atx* (#ATX 20 and #ATX 21) founders passed the transgene through the germ line. Transgenic mice were bred to activate the MMTV-LTR promoter, which contains hormonally responsive elements activated by progestins and corticosteroids (Ma et al., 1999). Real-time quantitative PCR analysis demonstrated expression of the *atx*, *lpa1*, *lpa2*, or *lpa3* transgenes in mammary glands of multiparous female mice (day 18 of second pregnancy; Figure 1C) with much higher levels than in virgin transgenic mice. Each of the LPA receptors and ATX were expressed in transgenic mammary glands of multiparous mice according to western blotting (Figure 1D). A weak band was detected with the ATX antibody in WT mice, likely representing endogenous ATX (Figure 1D, upper panel). Transgene expression was also detectable in spleen, intestine, lung, and uterus, albeit at much lower levels than in mammary glands (Figure 1D), consistent with the reported expression of the MMTV-LTR promoter (Sinn et al., 1987; Romieu-Mourez et al., 2003). To determine whether mammary epithelial-specific expression of LPA receptor or ATX perturbed normal mammary gland development, we performed whole mount analyses on mammary glands of 3- to 12-week-old virgin female transgenic mice. Transgenic mammary glands showed a slight increase in side branching, compared with WT females, including FVB/N and nontransgenic littermates (Figure 2). MMTV-*lpa1*, -*lpa2*, -*lpa3*, or MMTV-*atx* mice did not exhibit mammary gland abnormalities during gestation, were able to nurse pups, and gave birth to multiple litters of expected size. Thus, expression of LPA receptors or ATX does not appear to significantly alter mammary gland development and function.

MMTV-*lpa or* MMTV-*atx* Transgenic Mice Develop Chronic Mastitis, Hyperplasia, Mammary Intraepithelial Neoplasia, and Invasive and Metastatic Tumors

Multiparous (3 times) and virgin female as well as male mice from at least two different lines from the ATX, LPA1, LPA2, and LPA3 transgenic strains were monitored for tumor development over 24 months, When the presence of a palpable mammary lesion was detected or mice reached 24 months of age, mice were subjected to detailed histopathological analysis by a veterinary

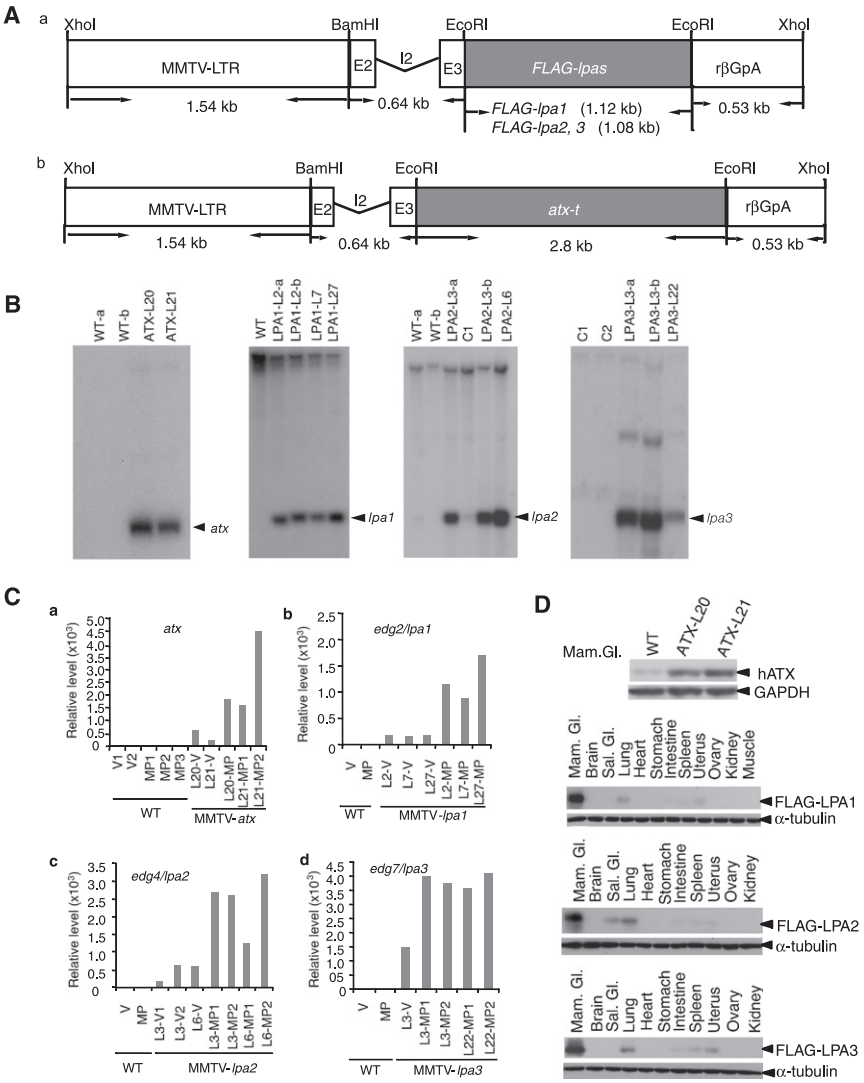

Figure 1. Generation and Characterization of Transgenic Mice

(A) The MMTV-*lpa1*, *-2*, or *-3* (a) or MMTV-*atx* (b) transgenic constructs contain the 1.54 kb MMTV-LTR and the full-length cDNA of FLAG-tagged human LPA receptors or full-length human *atx* linked to the KCR fragment containing the exon II (E2), intron II (I2), exon III (E3), and polyadenylation signal (rβGpA) derived from rabbit β-globin.

(B) Southern analysis of BamHI/XhoI-digested genomic DNA (15 μg) from potential founder mice hybridized with full-length human *lpa1*, *-2*, or *-3* cDNA probes or StuI/EcoRI fragment of human *atx*, genomic DNA from wild-type FVB/N (WT), or other strain of *edg* family as control (C1, LPA1; C2, LPA2) for MMTV-*lpas*.

(C) ATX or LPA receptor transgene RNA expression in mammary glands of virgin (V) and multiparous mice (MP, at day 18 of the second pregnancy) from different lines (L) were analyzed by real-time quantitative PCR.

(D) ATX or LPA receptor protein in transgenic mice. mammary gland (Mam. Gl), salivary gland (Sal. Gl).

pathologist (L.C.S.). No mammary cancers, including mammary intraepithelial neoplasia (MIN), were observed in a cohort of 44 multiparous WT mice, including FVB/N and nontransgenic littermates, consistent with reported low mammary tumor incidence (<1%) in FVB/N mice (Sinn et al., 1987; Romieu-Mourez et al., 2003). Furthermore, no mammary cancers were observed in virgin or male transgenic mice (data not shown).

Strikingly, the expression of ATX or LPA1, LPA2, or LPA3 receptors in the mammary gland of at least two independent lines for each of the transgenes of multiparous mice was sufficient to result in high frequency, albeit late-onset (ranging from 8 months to 24 months) mammary carcinomas with variable incidence (Figure 3). There were varying frequencies of abnormal proliferation (hyperplasia), noninvasive tumor formation (MIN), invasive mammary carcinoma, and metastasis to other organs among the transgenic mice (Figure 4). There was a low incidence of mastitis and mammary gland hyperplasia in nontransgenic mice at 22 months of age and over. In contrast, mammary glands from MMTV-*lpa* receptor and MMTV-*atx* mice demonstrated a high frequency and early onset of chronic mastitis indicative of chronic inflammation prior to development of tumors (Figure 4).

The incidence of mammary carcinoma was highest in *lpa2* (52.8%) transgenic mice with the earliest onset (average 16.5 months). In *lpa1* transgenic mice, the incidence of mammary carcinoma was the lowest (32.0%), with an average onset of 18.9 months. The incidence in *lpa*3 transgenic mice was 42.3%, with the longest tumor-free period (average 19.5 months). Fifty percent of *atx* transgenic mice developed mammary carcinoma at an average age of 20 months (Figure 3). The metastatic rate was highest in *lpa*3 (45.5%) transgenic mice with lower levels in other strains (Figure 4). Independent of strain, the sites of metastasis were regional lymphoma nodes (70%) and lung (30%), while no metastatic bone tumors were observed. The tumors encompassed adenocarcinomas (37.9%), adenosquamous carcinomas (19.5%), or combined adenocarcinoma and adenosquamous carcinoma (13.8%) with a major adenomatous component (total 71.2%), with MIN (14.9%), and with other histologies including carcinosarcoma and anaplastic carcinoma (13.9%) accounting for the remainder (see Figure S3 for representative histology). All mammary carcinomas and metastatic carcinomas assessed exhibited detectable levels of RNA (Figure S4A) and protein (Figure S4B) for each of the transgenes, although at variable levels.

Estrogen Receptor Expression in Mammary Carcinomas

Most murine transgenic models are estrogen receptor (ER) negative, limiting their applicability to the largest class of human breast cancers, which are ER positive. We thus assessed the effect of LPA receptors and ATX on ER expression in normal mammary glands and tumors. As indicated in Figure 5A, in the

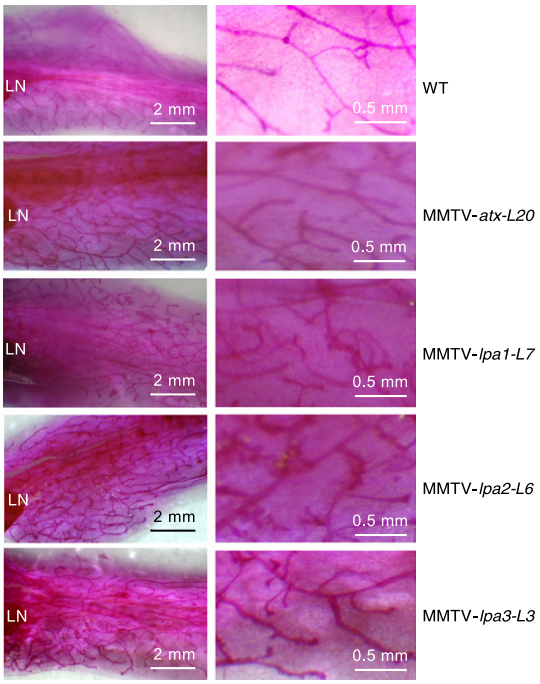

Figure 2. Effect of Transgene Expression in Virgin Murine Mammary Glands

Whole-mount analyses of the fourth inguinal mammary glands of 8-week-old virgin mice. Results are representative images from six mice of each group. The right column is magnification of the left column. LN indicates lymph node.

WT mammary gland, 10%–15% of the epithelial cells are ER positive compatible with previous studies (Figure 5A; Clarke et al., 1997; Zhang et al., 2005). Strikingly, in the transgenic mice assessed, the fraction of ER-positive cells, including nuclear ER-positive cells, was markedly enhanced in the mammary gland, especially in mammary ductal hyperplasias, with 40%–60% ER-positive cells (Figure 5A). A subset of both primary and metastatic tumors from transgenic mice had high ER levels, which was localized to the nucleus (Figure 5B). As with tumor development and metastases, there was marked variability in the fraction of tumors expressing ER (*atx*, 62.5%; *lpa1*, 23.0%; *lpa2*, 21.8%; and *lpa3*, 47.3%).

Expression of ATX and LPA Receptors Is Associated with Increased Cytokine Production

We have demonstrated that LPA is a potent inducer of IL-8 and vascular endothelial growth factor (VEGF) (Hu et al., 2001; Fang et al., 2004; Yu et al., 2008). Serum levels of both macrophage inflammatory protein 3 alpha (MIP-3α, murine equivalent of IL-8) and VEGF were significantly elevated in transgenic mice with mammary tumors (Figure 6). Intriguingly, in transgenic mice prior to tumor development, there was a small but consistent increase in MIP-3α and VEGF plasma levels, suggesting that the increase in plasma MIP-3α and VEGF precedes tumorigenesis (Figure 6). Whether the increase in MIP-3α and VEGF represents a consequence of the inflammatory process associated with the chronic mastitis present in the mice (Figure 4) or production of MIP-3α and VEGF by the increased number of epithelial cells expressing ATX or LPA receptors will require further evaluation.

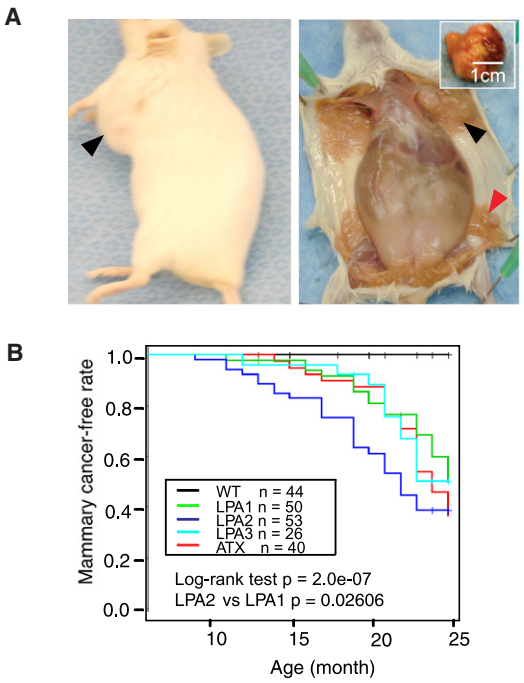

Lines	WT: FVB/N	WT: Nontransgenic littermates	LPA1: LPA1-L2	LPA1: LPA1-L7	LPA1: LPA1-L27	LPA2: LPA2-L3	LPA2: LPA2-L6	LPA3: LPA3-L3	LPA3: LPA3-L22	ATX: ATX-L20	ATX: ATX-L21
Cancer	0	0	4	3	9	13	15	10	1	13	7
No cancer	24	20	15	7	12	12	13	13	2	8	12
Subtotal	24	20	19	10	21	25	28	23	3	21	19
Total	44		50			53		26		40	
Cancer rate	0%		32.0%			52.8%		42.3%		50.0%	

Figure 3. Mammary Cancer Incidence in Female MMTV-*atx*, or MMTV-*lpa1*, *2*, or *3* Transgenic Mice

Female transgenic mice were bred 3 times to induce the MMTV-LTR promoter and monitored for tumor incidence over 24 months with WT females including FVB/N and nontransgenic littermates as controls.

(A) Mammary cancers, large (1.5 × 2.0 × 1.6 cm, black arrowhead) and small (0.5 × 0.5 × 0.5 cm, red arrowhead), developed in MMTV-*lpa2*.

(B) Kaplan-Meyer analysis of mammary cancers.

(C) Mammary cancer incidence in each line.

Effects of Transgene Expression on Cellular Signaling Pathways

To elucidate effects of transgenic expression of ATX and LPA receptors on signaling processes that could contribute to tumor initiation or progression, we used an emerging technology, reverse phase protein arrays (RPPA). WT and transgenic mammary gland and tumors from transgenic mice were assessed for presence or absence of tumor by histology by

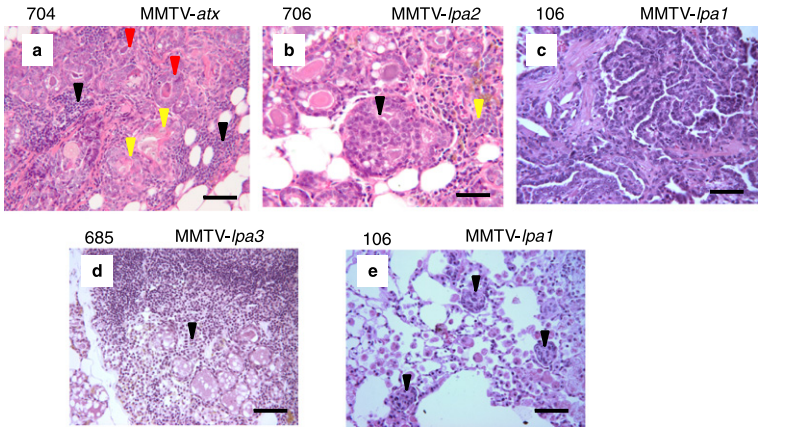

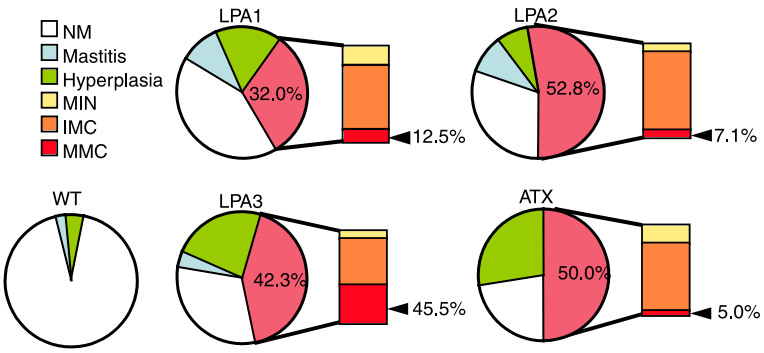

		LPA1			LPA2		LPA3		ATX	
	WT	Line 2	Line 7	Line 27	Line 3	Line 6	Line 3	Line 22	Line 20	Line 21
NM	41	9	3	9	7	9	7	1	4	5
Mastitis	1	2	3	0	1	4	1	0	0	0
Hyperplasia	2	3	3	2	3	1	5	1	1	10
MIN	0	0	0	3	2	1	0	0	1	3
IMC	0	3	2	6	10	13	6	0	11	4
MMC	0	1	0	1	2	0	4	1	1	0
Cancer	0/44 (0%)	16/50 (32.0%)			28/53 (52.8%)		11/26 (42.3%)		20/40 (50.0%)	
Metastasis	0/0 (0%)	2/16 (12.5%)			2/28 (7.1%)		5/11 (45.5%)		1/20 (5.0%)	

Figure 4. Spectrum of Mammary Gland Lesions

(A) Histopathology of mammary gland lesions in MMTV-*lpas* or MMTV-*atx* transgenic mice. (a) Chronic mastitis with white blood cell infiltration (black arrowhead) and squamous metaplasia (yellow arrowhead) of hyperplastic ducts (red arrowhead). (b) Mammary intraepithelial neoplasia (MIN) (black arrowhead) with hyperplastic ducts (yellow arrowhead) and chronic mastitis. (c) Invasive mammary adenocarcinoma. (d) Lymph node metastatic carcinoma (black arrowhead). (e) Lung metastatic carcinoma (black arrowhead) with pneumonia (scale, 50 μm).

(B) Representative mammary gland lesion histopathology. NM, normal mammary gland; Mastitis, chronic mastitis with squamous metaplasia; Hyperplasia, hyperplasia (with chronic mastitis); MIN, mammary intraepithelial neoplasia (with chronic mastitis and hyperplasia); IMC, invasive mammary carcinoma (with mastitis, hyperplasia or MIN); MMC, metastatic mammary carcinoma.

a veterinary pathologist (L.C.S.). On the basis of unsupervised hierarchical clustering, WT mammary glands and a number of transgenic mammary glands form a cluster at the bottom of the dendrogram (Figure 7A; for a sample list, see Table S1). A middle cluster is composed primarily of transgenic mammary glands with a subset of transgenic mammary tumors. The upper cluster is highly enriched for transgenic mammary cancers (Figure 7A). Thus, there appears to be a spectrum of proteomic changes from normal through transgenic mammary gland to mammary cancer.

Normal mammary glands exhibited relatively high levels of ER, PR, GATA3, and BCL2 compatible with functional ER signaling. Relatively high levels of phosphorylation of the EGFR, HER2, MKK3, MKK4, Stat1, and Stat6 are also present in normal epithelium. Furthermore, both p53 and phospho-p53 are present at higher levels in normal tissues than in tumor tissues. In contrast, mammary tumors demonstrated activation of the PI3K pathway, as indicated by phosphorylation of AKT, GSK3, mTOR, S6, and NF-κB with marked activation in a subset of tumors. Intriguingly, PTEN levels were increased in the transgenic tumors despite increases in signaling through the PI3K pathway (Figure 7A; Figure S5). The coordinate increase in AKT levels in the transgenic tumors as well as LPA receptor activation could bypass the effects of elevated PTEN. Alternatively, the increase in PTEN levels could be part of a feedback loop generated by activation of the PI3K pathway. Increased phosphorylation was also observed in components of the MAPK pathways (MAPK, p38, and ATF-2) as well as other targets, including Stat3 and PKCα. A number of components of the Wnt pathway implicated in cell invasion and metastases, including β-catenin, cyclin D1, and c-Jun were elevated in of the mammary tumors, as well as E-cadherin, an important contributor to inflammatory breast cancer (Kleer et al., 2001) (Figure 7A; Figure S5).

Two of the transgenic tumors clustered with normal mammary tissue (LPA2-3 MC16 and LPA3-3 MC8). This could be due to limited amounts of tumor present resulting from stromal contamination. However, phosphorylation of AKT, GSK3, MAPK, NF-κB, and ATF-2 was increased in LPA2-3 MC16, whereas phosphorylation of p38 and c-Jun was increased in LPA3-3 MC8, suggesting that signaling pathways were perturbed in these tumors. The RPPA data were utilized to direct a series of western blotting and IHC studies. Increased p38, MAPK, ATF-2, PKCα, AKT, GSK3,

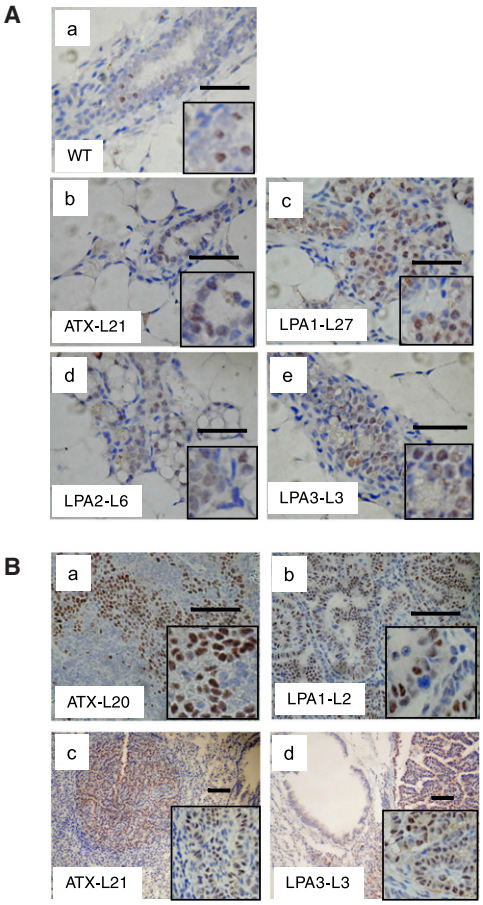

Figure 5. ER Expression in Mammary Glands and Mammary Carcinomas from MMTV-*lpas* or MMTV-*atx*

Paraffin sections of mammary carcinomas or mammary glands from adult transgenic mice (20–22 months old and multiparous) were assessed for ER by immunohistochemical staining, with normal mammary glands from WT multiparous mice as control (including FVB/N and nontransgenic littermates).

(A) ER expression in mammary glands of wild-type FVB (a), transgenic mice (b), or mammary ductal hyperplasia (c–e), (scale 50 μm).

(B) ER expression in tumors. (a) Mammary adenocarcinoma from MMTV-*atx*; (b) Mammary adenocarcinoma from MMTV-*lpa1*; (c) Mammary lymph node metastatic adenocarcinoma from MMTV-*atx*; (d) Lung metastatic adenocarcinoma from MMTV-*lpa3* (scale, 100 μm).

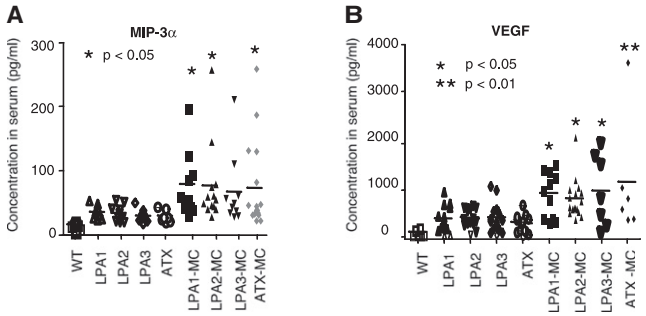

Figure 6. MIP-3α and VEGF Production in MMTV-*atx* or MMTV-*lpa1*, -*2*, or -*3* Mice

Serum MIP-3α and VEGF in transgenic mice with and without mammary carcinoma (MC) were quantified using MIP-3α and VEGF ELISA Kit. MIP-3α and VEGF concentrations were calculated by comparing the absorbance of samples to standard curves.

(A) MIP-3α.

(B) VEGF.

and S6 phosphorylation was readily observed by western blotting (Figure 7B) and β-catenin by IHC in the transgenic tumors (Figure 7C). The majority of the tumors assessed by western blotting are represented in the top cluster in Figure 7A, likely because of larger tumors being used to produce sufficient protein for western blotting. This likely contributes to the high levels of phosphorylation observed in Figure 7B. We used the RPPA to compare the transgenic ATX and LPA receptor mammary cancers with MMTV-*ErbB2*, MMTV-*Wnt1*, MMTV-CD8-*IGFIR*, MMTV-*IRS-1*, and MMTV-*IRS-2* transgenic mammary cancers on the same genetic background (Figure S6). Compared with the other transgenic tumors, the ATX and LPA receptor transgenic tumors demonstrated fewer changes in the targets assessed. Intriguingly, PTEN levels were elevated across all of the tumor lineages despite increased signaling through the PI3K pathway, as indicated by increased S6 phosphorylation (Figure S6). Compared with other transgenic lines, a subset of the ATX, LPA1, LPA2, and LPA3 tumors demonstrated elevated levels of phospho-ER, ER, PR, and GATA3 (Figure S6), compatible with retention of ER function in a subset of transgenic tumors (Figure 5). In terms of validating the proteomics approach, both HER2 and phospho-HER2 were markedly elevated in MMTV-*ErbB2* transgenic mice.

ATX and LPA Receptor Transgenic Mice Do Not Form a Distinct Group on Transcriptional Profiling

Compared with transcriptional profiles of 13 different murine transgenic mammary cancer models (Herschkowitz et al., 2007), the ATX and LPA receptor mammary tumors failed to form distinct clusters, but rather were scattered throughout the different mammary tumor models (Figure S7). Furthermore, several of the ATX and LPA receptor transgenic tumors clustered most closely (but distinct from) to normal mammary glands. Thus, the proteomics and transcriptional profiling data are consistent and compatible with a model wherein the ATX and LPA receptor transgenes allow accumulation of secondary mutations leading to late onset mammary cancers.

DISCUSSION

In this study, we demonstrate that expression of ATX and each of the *edg* family of LPA receptors sensitizes to initiation and progression of breast cancer. This finding, combined with the observations that LPA1 and LPA2 receptors are aberrantly expressed in breast cancers (Kitayama et al., 2004; Horak et al., 2007) and that LPA2 and LPA3 receptor levels correlate with tumor grade (Figure S1B), provides evidence supporting the contention that aberrant expression of LPA receptors or the enzyme producing LPA could contribute to the initiation and progression of human breast cancer. Importantly, these transgenic models, combined with the observation that inhibition of ATX or LPA receptors decrease metastases in human xenograft models (Boucharaba et al., 2006; Baker et al., 2006) as well as the development of ATX and LPA receptor inhibitors (Murph

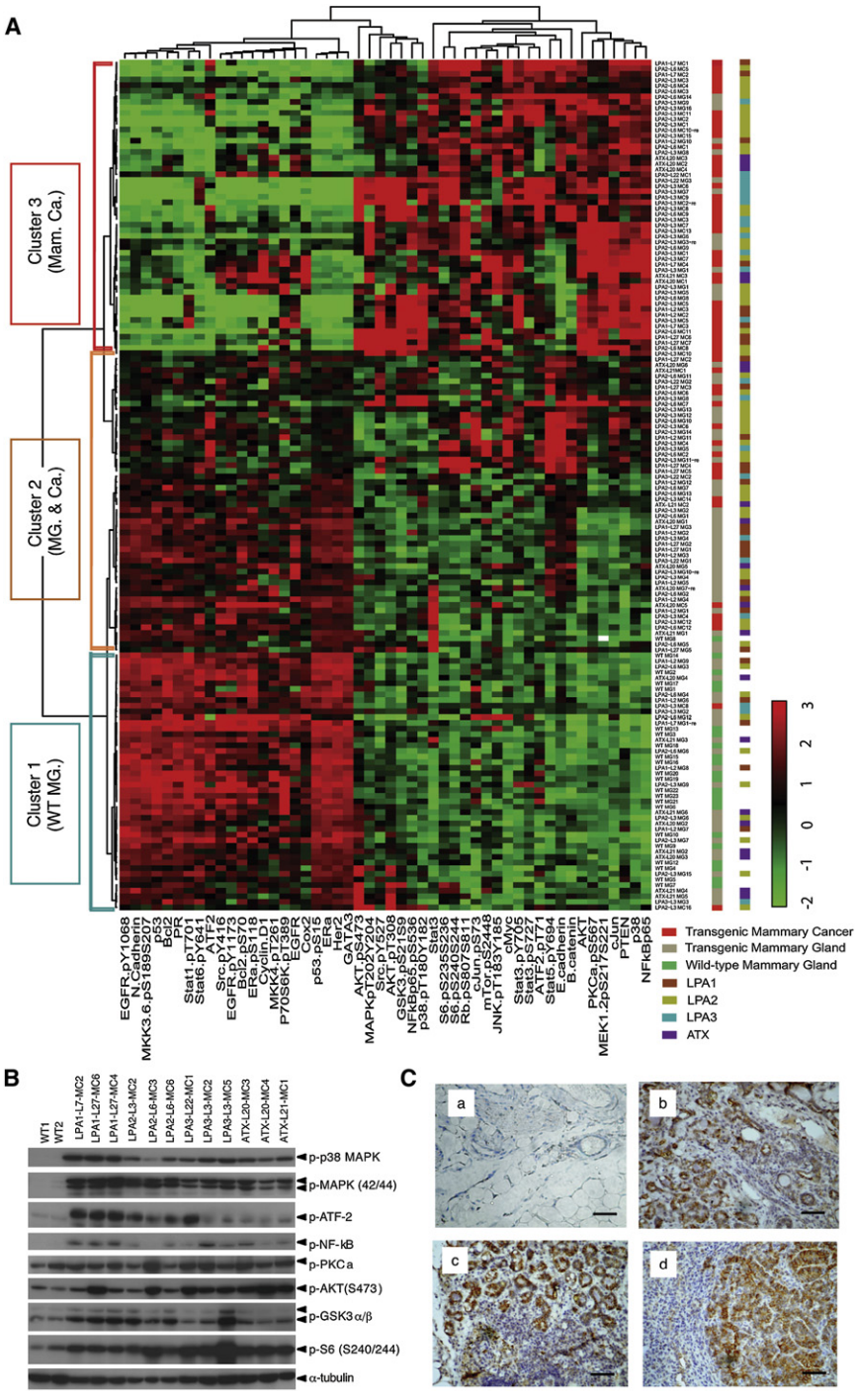

Figure 7. Effects of Transgene Expression on Cellular Signaling Pathways

(A) Variation in expression or phosphorylation of 50 proteins in 152 experimental samples from 145 mice. Data are presented in a matrix format: each row represents an experimental sample, and each column an antibody target. In each sample, the ratio of the abundance of the molecule to its median abundance across all tissue samples is represented by the color of the corresponding cell in the matrix (see scale, for expression levels). Dendrogram on left shows similarities in the expression patterns between experimental samples.

(B) Phosphorylation of p38-MAPK, ERK/MAPK, ATF-2, NF-κB, pPKCα, AKT, GSK3α/β, and S6 in mammary carcinomas (MC) from MMTV-*atx* and MMTV-*lpa1*, *-2*, *-3* mice was analyzed by western blot.

(C) Immunohistochemistry was performed on paraffin-embedded mammary carcinoma sections. Specimens were blocked and incubated with rabbit polyclonal antibody to β-catenin (detailed in Experimental Procedures). β-catenin expression in normal mammary gland of wild-type female mice (a); mammary adenocarcinoma from MMTV-*lpa2* (b); and mammary lymph node metastatic adenocarcinoma from MMTV-*lpa2* and MMTV-*atx* (c and d) (scale, 50 μm).

and Mills, 2007), establish ATX and LPA receptors as potential targets for therapy in human breast cancer and provide models to evaluate the efficacy of therapeutic interventions.

A recent study indicates that LPA1, LPA2, and LPA4 but not LPA3 are sufficient to induce transformation of MEF expressing myc and Tbx2 (Taghavi et al., 2008). The transformation of the MEF is associated with prolonged activation of signaling induced by LPA1, LPA2, and LPA4 but not LPA3. In contrast, LPA3 is sufficient to sensitize mammary epithelium to tumorigenesis and induces similar effects on cell signaling in the mammary tumors to LPA1 and LPA2. The differences in effects of LPA3 on tumorigenesis in the two models could be due to differential sensitivity of mammary epithelium and MEF to transformation or alternatively to an interaction between LPA3 and the microenvironment in the transgenic mammary model that is not recapitulated in the MEF in vitro.

Expression of each of ATX, LPA1, LPA2, or LPA3 was sufficient to induce late-onset mammary cancers in at least two lines for each transgene. Indeed, all of the lines that passed the MMTV-driven transgenes through the germline developed mammary tumors. The induction of tumors required activation of the MMTV promoter with multiple pregnancies. Furthermore, tumors were not observed in male or virgin transgenic mice or nontransgenic littermates. Thus, it is highly unlikely that the mammary tumors occur as a result of integration of the transgenes into other loci but rather represent an effect of expression of ATX and LPA receptors on the initiation or progression of mammary tumors.

We have demonstrated that the *edg* family of LPA receptors is pleiomorphic in function (Yu et al., 2008). Indeed, although each of the LPA receptors preferentially links to particular pathways and functional outcomes, the receptors retain the capability of

inducing similar signaling events and functional outcomes (Yu et al., 2008). Alternatively, by increasing cell viability, one of the major activities of LPA, ATX and the LPA receptors could increase the likelihood that mutations acquired over prolonged latent period would lead to tumor development. Indeed, the ATX and LPA receptor driven tumors (Figure S7 and data not shown), do not form a distinct cluster on functional proteomics or transcriptional profiling and indeed demonstrate fewer aberrations than most transgenic models clustering closest to, but distinct, from normal mammary glands. This is compatible with LPA production and function increasing the susceptibility of mammary epithelium to a spectrum of secondary transforming events.

As the major effect of ATX in vivo appears to be production of LPA (Van Meeteren et al., 2006; Pamuklar et al., 2009), the ability of ATX to increase tumorigenesis suggests that mammary epithelial cells express functional LPA receptors and are able to respond to LPA. Indeed both human mammary epithelial cells and normal murine mammary glands express LPA1, LPA2, and LPA3, albeit with low levels of LPA2 in murine mammary glands (Figures S1 and S2). Intriguingly, increasing circulating LPA levels by two fold by driving ATX expression by alpha-1-antitrypsin (liver specific expression) is not sufficient to induce mammary tumorigenesis (Pamuklar et al., 2009; data not shown) and further circulating LPA levels are not elevated in the MMTV-*ATX* transgenic mice (data not shown). Unfortunately, there are no feasible approaches to determine the concentration of ATX in the interstitial fluid so we are unable to determine the level of LPA at the cell surface of the mammary epithelial cells. However, the increased tumorigenesis in the ATX transgenic mice suggests that local production of LPA due to increased ATX levels is sufficient to sensitize mammary epithelium to transformation. Enforced expression of LPA receptors in MEF (Taghavi et al., 2008) or human ovarian cancer cells (Yu et al., 2008) is not sufficient to induce ligand-independent signaling, but rather renders the cells more sensitive to extracellular LPA and, in particular, prolongs cellular signaling. Thus, the increased tumor development in the LPA receptor strains suggests that either LPA is produced locally, or that circulating LPA (nM) is sufficient to activate the transgenic LPA receptors.

Current biological, transcriptional profiling and clinical approaches have classified human ductal carcinomas into 3 major subtypes: ER positive, HER2 amplified, and triple negative or ''basal'' tumors which lack ER, PR, and HER2 expression (Herschkowitz et al., 2007). The ''triple negative'' or basal tumors are well represented in transgenic models and multiple transgenic and knock-in HER2 tumors models are available; however, there are few ER-positive transgenic mouse models, particularly models that are invasive and metastatic, limiting therapeutic and functional characterization of this important type of cancer. Aberrant expression of LPA receptors and ATX enhanced ER expression in mammary glands, and many of the resultant mammary cancers were ER positive, including metastatic tumors. Furthermore, a fraction of the transgenic tumors demonstrated nuclear ER staining as well as elevated phospho-ER, PR, GATA3, and BCL2, compatible with functional ER signaling. Together, the data suggest that these transgenic mouse models have the potential to mimic human breast cancer. Functional proteomic analysis of the transgenic tumors demonstrated that both p38-MAPK and ERK/MAPK were activated in a subset of the transgenic mammary cancers, particularly in larger tumors. LPA activates p38-MAPK, ERK/MAPK pathways, inducing cancer cell invasion in vitro (Estrella et al., 2007; Hao et al., 2007), compatible with the metastatic capacity of the transgenic tumors. An activated MAPK pathway, particularly in concert with PI3K pathway activation, increases expression of ATF-2 and NF-κB, two master inflammatory transcription factors (Bhat et al., 2002; Patel et al., 2007). Indeed, both phosphorylated ATF-2 and NF-κB were present in a subset of the mammary tumors (Figures 7A and 7B). Activation of ATF-2 and NF-κB can induce cytokine production (Panne et al., 2007; Balkwill et al., 2005), compatible with the increases in MIP-3α and VEGF in the serum of transgenic mice prior to the development of tumors and the marked increases after tumor development (Figure 6). The increases in MIP-3α and VEGF are consistent with our demonstration that overexpression of the *edg* family of LPA receptors enhances LPA-induced production of cytokines, while silencing expression of the LPA receptors decreases cytokine production (Yu et al., 2008). These cytokines may subsequently activate signal transducer and activator of transcription (Stat) family members contributing to inflammation and tumor formation (Wegenka et al., 1994; Bromberg et al., 1999; Li et al., 2007). Indeed, phosphorylation of both Stat3 and Stat5 were increased in a subset of the transgenic mammary tumors (Figure 7; Figure S5). The LPA receptor and ATX transgenic mice demonstrated a high frequency of chronic inflammation, as indicated by mastitis, prior to the development of MIN or malignancies. Furthermore, both the local and metastatic tumors were associated with a significant degree of lymphocytic infiltration. Thus, inflammation may contribute to the development of mammary cancers in the transgenic mice. In a significant proportion of the murine tumors, the PI3K/AKT (protein kinase B) pathway, which is implicated in breast cancer through frequent mutational activation and increases in phosphorylation of AKT in tumors, is up-regulated. The PI3K/AKT pathway has been implicated in the development of resistance to endocrine therapy in breast cancer cell lines and in the response to herceptin (Hennessy et al., 2005; Berns et al., 2007), suggesting that ATX and LPA receptors may contribute to therapy resistance as well as tumorigenesis, invasion, and metastases. LPA decreases p53 levels through activation of the PI3K-AKT pathway (Murph et al., 2007; Aylon and Oren, 2007). The decrease in expression and phosphorylation of p53 in the transgenic tumors suggests that deficient p53 function could contribute to tumor development or progression to metastases (Hollstein et al., 1991; Bosco and Knudsen, 2007). LPA induces the accumulation of β-catenin and induces the proliferation of colon cancer–derived cell lines through activation of LPA2 and LPA3 (Yang et al., 2005). Compatible with this observation, β-catenin levels and potential downstream effectors of the Wnt pathway, including c-Jun and cyclin D1, were increased in a fraction of the transgenic mammary carcinomas. The increases in c-Jun and cyclin D1 are likely not mediated solely through Wnt signaling, because the PI3K and MAPK pathways (Dearth et al., 2006), which are activated in the transgenic mammary tumors, contribute to regulation of c-Jun and cyclin D1.

In summary, aberrant expression of each of the *edg* family of LPA receptors or the LPA producing enzyme, ATX, in mammary

glands is sufficient to sensitize transgenic mice to the initiation and progression of breast cancer. Strikingly, the resultant tumors showed a broad range of histotypes, with inflammation and metastatic properties, and were positive or negative for the ER, mimicking human breast cancer. These transgenic models should provide powerful tools for the understanding of the pathophysiology of breast cancer and for the development and implementation of effective breast cancer therapeutics.

EXPERIMENTAL PROCEDURES

Plasmid Construction

To generate a mammary gland transgenic vector containing FLAG-tagged LPA receptors or ATX, we used MMTV-KCR (BS) (S. Tsai, Baylor College of Medicine, Houston, TX). *FLAG-lpa1*, *-2*, and *-3* were transferred from pcDNA3.0-*FLAG-lpa1*, *-2*, and *-3* plasmids, containing the FLAG-tagged full-length human *lpa1*, *-2*, or *-3* cDNA, into pCR II vector with a TA cloning kit (Invitrogen). After sequence verification, the pCR II *FLAG-lpa1*, *-2*,or *-3* vectors were digested with EcoRI (for *FLAG-lpa1*, with partial digestion) to generate *FLAG-lpa1*, *-2*, or *-3* fragments, which were cloned into the EcoRI site of MMTV-KCR (BS) to generate MMTV-KCR-*FLAG-lpa1*, *-2*, or *-3*. The direction of the inserts was confirmed by restriction mapping and DNA sequencing. The MMTV-KCR-*FLAG-lpa1*, *-2*, and *-3* plasmids were excised to generate MMTV-KCR- *FLAG-lpa1* (3.83 kb), MMTV-KCR- *FLAG-lpa2*, or MMTV-KCR-*FLAG-lpa3* (3.79 kb) vector-free fragments, containing long terminal repeats (MMTV-LTR), which directs expression to the mammary epithelium. FLAG-tagged *LPA1*, *-2*, or *-3*; the partial exon II, intron II, and exon III; and a endogenous polyadenylation signal derived from the rabbit β-globin gene (Ma et al., 1999) were used to generate transgenic mice. We used the same method to prepare MMTV-KCR-*atx* (5.3 kb), which includes the MMTV-LTR sequence, full-length human *atx* cDNA, rabbit β-globin intron, and poly(A) signal sequence.

Generation of Transgenic Mice

The MMTV-KCR- *FLAG-lpa1*, *-2*, or *-3* or *MMTV-KCR-atx* fragments were gel purified and microinjected into pronuclei of single-cell embryos isolated from FVB/N mice in the Genetically Engineered Mouse Facility CCSG core. Zygotes were implanted into pseudopregnant foster mothers. Offspring were screened for presence of the transgene using PCR to amplify the region spanning the FLAG-tagged *lpa1*, *-2*, or *-3* or human *atx* transgene. The sequence of forward primer for *lpa1, lpa2, and lpa3* is located in FLAG-tag, ATGGACTA CAAGGACGACGATG. The sequences of reverse primers are LPA1-reverse, CTAAACCACAGAGTGGTCATTG; LPA2-reverse, CTAAAGGGTGGAGTCCAT CAG; and LPA3-reverse, GGAAGTGCTTTTATTGCAGAC. The *atx* primers are ATX-forward, CCCAGAAATCCTGACACTCA and ATX-reverse, CCCATAT GTCCTTCCGAGTG. Southern hybridization with 15 μg of tail DNA digested with BamHI/XhoI, and probed with full-length *lpa1*, *-2*, or *-3* cDNA or the StuI/EcoRI fragment of ATX as probe was used to confirm founders. Transgenic mice were bred (with nontransgenic littermates and FVB/N WT mice) to establish 3 independent transgenic lines of MMTV-*lpa1* and 2 lines of MMTV-*lpa2*, MMTV-*lpa3*, and MMTV-*atx*. MMTV-*lpa1*, *-2*, or *-3* were bred to be homozygous. For as yet unknown reasons, we were unable to create homozygous MMTV-*atx* mice. Female transgenic mice were bred three times to induce transgene expression though activation of the hormone-dependent MMTV-LTR promoter; WT FVB/N mice and nontransgenic littermates were bred using the same conditions. F4- and F5-generation mice were used for analysis at the RNA and protein level. All animal studies were carried out under IACUC approved protocols. Mice were monitored weekly for the appearance of tumors. All mice, whether or not their tumors were obvious, were submitted for detailed pathological analysis. Transgenic mice indicated as tumor free did not have detectable tumor masses or tumors on histological analysis. MMTV-*ErbB2*, MMTV-*CD8-IGF-IR*, MMTV-*IRS1*, MMTV-*IRS2*, and MMTV-*Wnt1* mice were bred and genotyped as previously reported (Dearth et al., 2006; Carboni et al., 2005).

Real-time Quantitative PCR

Total RNA was isolated using RNeasy Protect Mini Kit (QIAGEN) according to the manufacturer's protocol. Taqman probes and Taqman One-Step RT-PCR master reagent were from Applied BioSystems. Human and mouse LPA1, -2, and -3 and ATX mRNA levels were determined by Taqman real-time RT-PCR using the ABI PRISM 7700 Sequence Detection System (Liu et al., 2008).

Whole Mount, Histology, and Immunohistochemistry

The left inguinal mammary gland was excised from 3- to 12-week-old virgin female transgenic mice and spread on glass slides for overnight fixation. The next day the samples were hydrated, stained overnight in Carmine, and then dehydrated, precleared in toluene, and stored in methyl salicylate. To prepare sections, specimens of mammary glands or tumors were fixed with 10% formalin for 24 hr, embedded in paraffin, and then sectioned at 5 μm thickness, followed by hematoxylin-eosin staining. For immunohistochemistry, specimens were blocked and incubated with rabbit anti-mouse polyclonal antibody to ERα (1:400, Santa Cruz Biotechnology; Santa Cruz, CA) or rabbit polyclonal antibody to β-catenin (1:50, Biosource, CA) at 4°C overnight, followed by incubation with goat anti-rabbit horseradish peroxidase-conjugated antibodies (1:500, Bio-Rad, Hercules, CA). Mayer's hematoxylin (Sigma) was used as a counter stain.

Measurement of MIP-3α and VEGF Production by ELISA

Serum MIP-3α and VEGF from WT and transgenic mice (18–22 months old) with and without mammary carcinoma (MC) were quantified by ELISA using MIP-3α and VEGF ELISA kits (R&D Systems). Concentrations were calculated by comparing the sample absorbance to standard curves.

Western Analyses

Protein extracts were prepared from frozen mammary tissues by homogenization in ice-cold X-100 lysis buffer (Liu et al., 2004). To assess FLAG expression, 5 μg of protein was separated by SDS PAGE and transferred to imobilon prior to blocking with 5% milk and incubating membranes with anti-FLAG M2 monoclonal antibody (Sigma) (1:7500), followed by goat anti-mouse horseradish peroxidase-conjugated antibodies (1:10,000) (Bio-Rad, Hercules, CA). α-Tubulin was purchased from Cell Signaling (Beverly, MA); other antibodies are listed in Table S2.

Transcriptional Profiling

RNA was isolated from MMTV-*lpa1*, MMTV-*lpa2*, MMTV-*lpa3*, and MMTV-*atx* (5 of each strain) mammary tumors using QIAGEN RNAeasy kit according to the manufacturer's protocol, and were assessed using Agilent 4x44K murine arrays (Herschkowitz et al., 2007). The data were uploaded into the UNC Microarray Database where lowess normalization was performed. The data from the 20 new arrays were combined with 146 arrays from Herschkowitz et al. (2007) and DWD (Benito et al., 2004) was used to correct for microarray platform biases, followed by hierarchical cluster analysis using the mouse intrinsic gene set (Herschkowitz et al., 2007).

Reverse Phase Protein Array

The tissue lysates used for western blot were also used for reverse phase protein array (RPPA). Samples were mixed with buffer (35% glycerol, 8% SDS, 0.25 mol/L Tris HCl [pH 6.8], plus 10% β-ME without bromophenol blue) and were boiled for 5 min. Serial dilutions of samples were prepared, and diluted lysates were transferred to a 384-well plate, for printing with an automated robotic GeneTac arrayer (Genomic Solutions, Inc., Ann Arbor, MI) as described elsewhere (Zhang et al., 2007; Tibes et al., 2006). Slides were stained with an automated robot (BioGenex, San Ramon, CA). The antibodies used for RPPA are listed in Table S1.

Statistical Analyses

The RPPA-scanned slide images were quantified by MicroVigene software (version 2.9.9.7, VigeneTech Inc., Carlisle, MA). Spot signal intensities were processed by in-house software SuperCurve (version 0.997) (Hu et al., 2007), currently available as version 1.01 at the repository http://bioinformatics.mdanderson.org/OOMPA. Three replicate samples from the same lysate were averaged. Two sets of slides were run, and normalized data were combined using z-scores on each slide. Hierarchical clustering in the rows (samples) and the columns (antibodies) used the Euclidean distance and complete agglomeration in the heat maps. p values were obtained from a one-way ANOVA followed by Dunnett's test for each antibody. The F-test

p values from the ANOVA were adjusted by Benjamini-Hochberg method (Benjamini and Hochberg, 1995), for false discovery rate (FDR) control. Dunnett's test p values were reported only when the F-test was significant at FDR = 0.05. Mammary tumor free survival analysis was performed using the Kaplan-Meier method. Differences in survival were determined using log-rank test (Harrington and Fleming, 1982). Tumor incidence was compared between the genotype groups using Fisher's exact test (Fisher, 1935; Clarkson et al., 1993). The analyses were performed using R (version 2.6.2) (R Development Core Team, 2008).

ACCESSION NUMBERS

Microarray data described herein are available at the NCBI Gene Expression Omnibus (http://www.ncbi.nlm.nih.gov/geo/) under the accession number GSE15263.

SUPPLEMENTAL DATA

The Supplemental Data include two tables and seven figures and can be found with this article online at http://www.cell.com/cancer-cell/supplemental/S1535-6108(09)00115-9.

ACKNOWLEDGMENTS

We are grateful to S. Tsai (Baylor College of Medicine) for providing MMTV-KCR (BS) vector; K.W. Cheng (MD Anderson Cancer Center) for providing pcDNA3.0-*FLAG-lpa1*, *2*, and *3* vectors; D. Siwak (MD Anderson Cancer Center) for technical assistance on RPPA; T. Clair (National Cancer Institute) for providing pcDNA3.1-*atx/LysoPLD* vector; T.J. Aoki (The University of Tokyo) for providing anti-ATX antibody; and O. Britton (Breast Center, Baylor College of Medicine) for technical assistance on whole mount. The work was supported by DOD Breast Cancer Research Program DAMD17-03-1-0409 (to S.L.), by National Institute of Health Grants CA82716, CA64602, and CA099031 (to G.B.M.), and CA94118 (to A.V.L.), by a Breast Cancer Research Foundation Grant (to G.B.M.), by sponsored research to M.M. from LPATH Biotechnologies, and by National Institute of Health Core Grant P30 CA016672. Lpath Therapeutics, Inc. sponsored research to G.B.M. and M.M. G.B.M. is a stockholder in Lpath Therapeutics, Inc.

Received: August 20, 2008
Revised: January 5, 2009
Accepted: March 26, 2009
Published: June 1, 2009

REFERENCES

Aylon, Y., and Oren, M. (2007). Living with p53, dying of p53. Cell *130*, 597–600.

Baker, D.L., Fujiwara, Y., Pigg, K.R., Tsukahara, R., Kobayashi, S., Murofushi, H., Uchiyama, A., Murakami-Koh, E., Bandle, R.W., et al. (2006). Carba analogs of cyclin phophatidic acid are selective inhibitors of autotaxin and cancer cell invasion and metastasis. J. Biol. Chem. *281*, 22786–22793.

Balkwill, F., Charles, K.A., and Mantovani, A. (2005). Smoldering and polarized inflammation in the initiation and promotion of malignant disease. Cancer Cell *7*, 211–217.

Benito, M., Parker, J., Du, Q., Wu, J., Xiang, D., Perou, C.M., and Marron, J.S. (2004). Adjustment of systematic microarray data biases. Bioinformatics *20*, 105–114.

Benjamini, Y., and Hochberg, Y. (1995). Controlling the false discovery rate: a practical and powerful approach to multiple testing. J. R. Statist. Soc. B *57*, 289–300.

Berns, K., Horlings, H.M., Hennessy, B.T., Madiredjo, M., Hijmans, E.M., Beelen, K., Linn, S.C., Gonzalez-Angulo, A.M., Stemke-Hale, K., Hauptmann, M., et al. (2007). A functional genetic approach identifies the PI3K pathway as a major determinant of trastuzumab resistance in breast cancer. Cancer Cell *12*, 395–402.

Bhat, N.R., Feinstein, D.L., Shen, O., and Bhat, A.N. (2002). p38 MAPK-mediated transcriptional activation of inducible nitric-oxide synthase in glial cells. Roles of nuclear factors, nuclear factor kappa B, cAMP response element-binding protein, CCAAT/enhancer-binding protein-beta, and activating transcription factor-2. J. Biol. Chem. *277*, 29584–29592.

Bosco, E.E., and Knudsen, E.S. (2007). RB in breast cancer: at the crossroads of tumorigenesis and treatment. Cell Cycle *6*, 667–671.

Boucharaba, A., Serre, C.M., Gres, S., Saulnier-Blache, J.S., Bordet, J.C., Guglielmi, J., Clezardin, P., and Peyruchaud, O. (2004). Platelet-derived lysophosphatidic acid supports the progression of osteolytic bone metastases in breast cancer. J. Clin. Invest. *114*, 1714–1725.

Boucharaba, A., Serre, C.M., Guglielmi, J., Bordet, J.C., Clezardin, P., and Peyruchaud, O. (2006). The type 1 lysophosphatidic acid receptor is a target for therapy in bone metastases. Proc. Natl. Acad. Sci. USA *103*, 9643–9648.

Bromberg, J.F., Wrzeszczynska, M.H., Devgan, G., Zhao, Y., Pestell, R.G., Albanese, C., and Darnell, J.M., Jr. (1999). Stat3 as an oncogene. Cell *98*, 295–303.

Carboni, J.M., Lee, A.V., Hadsell, D.L., Rowley, B.R., Lee, F.Y., Bol, D.K., Camuso, A.E., Gottardis, M., Greer, A.F., Ho, C.P., et al. (2005). Tumor development by transgenic expression of a constitutively active insulin-like growth factor I receptor. Cancer Res. *65*, 3781–3787.

Chen, M., Towers, L.N., and O'Connor, K. (2007). LPA2 (EDG4) mediates Rho-dependent chemotaxis with lower efficacy than LPA1 (EDG2) in breast carcinoma cells. Am. J. Physiol. Cell Physiol. *292*, C1927–C1933.

Clarke, R.B., Howell, A., Potten, C.S., and Anderson, E. (1997). Dissociation between steroid receptor expression and cell proliferation in the human breast. Cancer Res. *57*, 4987–4991.

Clarkson, D.B., Fan, Y., and Joe, H. (1993). A remark on algorithm 643: FEXACT: an algorithm for performing Fisher's exact test in rxc contingency tables. ACM Trans. Math. Softw. *19*, 484–488.

Dearth, R.K., Cui, X., Kim, H.J., Kuiatse, I., Lawrence, N.A., Zhang, X., Divisova, J., Britton, O.L., Mohsin, S., Allred, D.C., et al. (2006). Mammary tumorigenesis and metastasis caused by overexpression of insulin receptor substrate 1 (IRS-1) or IRS-2. Mol. Cell. Biol. *26*, 9302–9314.

Desmedt, C., Piette, F., Loi, S., Wang, Y., Lallemand, F., Haibe-Kains, B., Viale, G., Delorenzi, M., Zhang, Y., d'Assignies, M.S., et al. (2007). Strong time dependence of the 76-gene prognostic signature for node-negative breast cancer patients in the TRANSBIG multicenter independent validation series. Clin. Cancer Res. *13*, 3207–3214.

Estrella, V.C., Eder, A.M., Liu, S., Pustilnik, T.B., Tabassam, F.H., Claret, F.X., Gallick, G.E., Mills, G.B., and Wiener, J.R. (2007). Lysophosphatidic acid induction of urokinase plasminogen activator secretion requires activation of the p38MAPK pathway. Int. J. Oncol. *31*, 441–449.

Fang, X., Gaudette, D., Furui, T., Mao, M., Estrella, V., Eder, A., Pustilnik, T., Sasagawa, T., Lapushin, R., Yu, S., et al. (2000). Lysophospholipid growth factors in the initiation, progression, metastases, and management of ovarian cancer. Ann. N Y Acad. Sci. *905*, 188–208.

Fang, X., Yu, S., Bast, R.C., Liu, S., Xu, H.J., Hu, S.X., LaPushin, R., Claret, F.X., Aggarwal, B.B., Lu, Y., et al. (2004). Mechanisms for lysophosphatidic acid-induced cytokine production in ovarian cancer cells. J. Biol. Chem. *279*, 9653–9661.

Finak, G., Bertos, N., Pepin, F., Sadekova, S., Souleimanova, M., Zhao, H., Chen, H., Omeroglu, G., Meterissian, S., Omeroglu, A., et al. (2008). Stromal gene expression predicts clinical outcome in breast cancer. Nat. Med. *14*, 518–527.

Fisher, R.A. (1935). The logic of inductive inference. J. R. Stat. Soc. Ser. A Stat. Soc. *98*, 39–54.

Hao, F., Tan, M., Xu, X., Han, J., Miller, D.D., Tigyi, G., and Cui, M.Z. (2007). Lysophosphatidic acid induces prostate cancer PC3 cell migration via activation of LPA(1), p42 and p38alpha. Biochim. Biophys. Acta. *1771*, 883–892.

Harrington, D.P., and Fleming, T.R. (1982). A class of rank test procedures for censored survival data. Biometrika *69*, 553–566.

Hennessy, B.T., Smith, D.L., Ram, P.T., Lu, Y., and Mills, G.B. (2005). Exploiting the PI3K/AKT pathway for cancer drug discovery. Nat. Rev. Drug Discov. *4*, 988–1004.

Herschkowitz, J.I., Simin, K., Weigman, V.J., Mikaelian, I., Usary, J., Hu, Z., Rasmussen, K.E., Jones, L.P., Assefnia, S., Chandrasekharan, S., et al. (2007). Identification of conserved gene expression features between murine mammary carcinoma models and human breast tumors. Genome Biology *8*, R76.

Hollstein, M., Sidransky, D., Vogelstein, B., and Harris, C.C. (1991). p53 mutations in human cancers. Science *253*, 49–53.

Horak, C.E., Mendoza, A., Vega-Valle, E., Albaugh, M., Graff-Cherry, C., McDermott, W.G., Hua, E., Merino, M.J., Steinberg, S.M., Khanna, C., et al. (2007). Nm23-H1 suppresses metastasis by inhibiting expression of the lysophosphatidic acid receptor EDG2. Cancer Res. *67*, 11751–11759.

Hu, J., He, X., Baggerly, K.A., Coombes, K.R., Hennessy, B.T.J., and Mills, G.B. (2007). Non-parametric quantification of protein lysate arrays. Bioinformatics *23*, 1986–1994.

Hu, X., Haney, N., Kropp, D., Kabore, A.F., Johnston, J.B., and Gibson, S.B. (2005). Lysophosphatidic acid (LPA) protects primary chronic lymphocytic leukemia cells from apoptosis through LPA receptor activation of the anti-apoptotic Protein AKT/PKB. J. Biol. Chem. *280*, 9498–9508.

Hu, Y.L., Tee, M.K., Goetzl, E.J., Auersperg, N., Mills, G.B., Ferrara, N., and Jaffe, R.B. (2001). Lysophosphatidic acid induction of vascular endothelial growth factor expression in human ovarian cancer cells. J. Natl. Cancer Inst. *93*, 762–768.

Ishdorj, G., Graham, B.A., Hu, X., Chen, J., Johnston, J.B., Fang, X., and Gibson, S.B. (2008). Lysophosphatidic acid (LPA) protected cancer cells from histone deacetylase (HDAC) inhibitor-induced apoptosis through activation of HDAC. J. Biol. Chem. *283*, 16818–16829.

Jemal, A., Siegel, R., Ward, E., Murray, T., Xu, J., and Thun, M.J. (2007). Cancer statistics. CA Cancer J. Clin. *57*, 43–66.

Kitayama, J., Shida, D., Sako, A., Ishikawa, M., Hama, K., Aoki, J., Arai, H., and Nagawa, H. (2004). Over-expression of lysophosphatidic acid receptor-2 in human invasive ductal carcinoma. Breast Cancer Res. *6*, R640–R646.

Kleer, C.G., van Golen, K.L., Braun, Y., and Merajver, S.D. (2001). Persistent E-cadherin expression in inflammatory breast cancer. Mod. Pathol. *14*, 458–464.

Li, Y., Du, H., Qin, Y., Roberts, J., Cummings, O.W., and Yan, C. (2007). Activation of the signal transducers and activators of the transcription 3 pathway in alveolar epithelial cells induces inflammation and adenocarcinomas in mouse lung. Cancer Res. *67*, 8494–8503.

Liu, S., Yu, S., Hasegawa, Y., LaPushin, R., Xu, H.J., Woodgett, J.R., Mills, G.B., and Fang, X. (2004). Glycogen synthase kinase 3 is a negative regulator of growth factor-induced activation of the c-Jun N-terminal kinase. J. Biol. Chem. *279*, 51075–51081.

Liu, S., Fang, X., Hall, H., Yu, S., Smith, D., Lu, Z., Fang, D., Liu, J., Stephens, L.C., Woodgett, J.R., and Mills, G.B. (2008). Homozygous deletion of glycogen synthase kinase 3beta bypasses senescence allowing Ras transformation of primary murine fibroblasts. Proc. Natl. Acad. Sci. USA *105*, 5248–5253.

Ma, Z.Q., Chua, S.S., DeMayo, F.J., and Tsai, S.Y. (1999). Induction of mammary gland hyperplasia in transgenic mice over-expressing human Cdc25B. Oncogene *18*, 4564–4576.

Moolenaar, W.H., van Meeteren, L.A., and Giepmans, B.N. (2004). The ins and outs of lysophosphatidic acid signaling. Bioessays *26*, 870–812.

Murph, M.M., and Mills, G.B. (2007). Targeting the lipids LPA and S1P and their signaling pathways to inhibit tumour progression. Expert Rev. Mol. Med. *9*, 1–18.

Murph, M.M., Hurst-Kennedy, J., Newton, V., Brindley, D.N., and Radhakrishna, H. (2007). Lysophosphatidic acid decreases the nuclear localization and cellular abundance of the p53 tumor suppressor in A549 lung carcinoma cells. Mol. Cancer Res. *5*, 1201–1211.

Ngan, E.S., Ma, Z.Q., Chua, S.S., DeMayo, F.J., and Tsai, S.Y. (2002). Inducible expression of FGF-3 in mouse mammary gland. Proc. Natl. Acad. Sci. USA *99*, 11187–11192.

Pamuklar, Z., Federico, L., Liu, S., Umezu-Goto, M., Dong, A., Panchatcharam, M., Fulkerson, Z., Berdyshev, E., Natarajan, B., Fang, F., et al. (2009). Autotaxin/lysophospholipase D and lysophosphatidic acid regulate murine hemostasis and thrombosis. J. Biol. Chem. *284*, 7385–7394.

Panne, D., Maniatis, T., and Harrison, S.C. (2007). An atomic model of the interferon-beta enhanceosome. Cell *129*, 1111–1123.

Patel, D.N., King, C.A., Bailey, S.R., Holt, J.W., Venkatachalam, K., Agrawal, A., Valente, A.J., and Chandrasekar, B. (2007). Interleukin-17 stimulates C-reactive protein expression in hepatocytes and smooth muscle cells via p38 MAPK and ERK1/2-dependent NF-kappaB and C/EBPbeta activation. J. Biol. Chem. *282*, 27229–27238.

R Development Core Team. (2008). R: A language and environment for statistical computing. http://www.R-project.org

Romieu-Mourez, R., Kim, D.W., Shin, S.M., Demicco, E.G., Landesman-Bollag, E., Seldin, D.C., Cardiff, R.D., and Sonenshein, G.E. (2003). Mouse mammary tumor virus c-rel transgenic mice develop mammary tumors. Mol. Cell. Biol. *23*, 5738–5754.

Sasagawa, T., Okita, M., Murakami, J., Kato, T., and Watanabe, A. (1999). Abnormal serum lysophospholipids in multiple myeloma patients. Lipids *34*, 17–21.

Schlyer, S., and Horuk, R. (2006). I want a new drug: G-protein-coupled receptors in drug development. Drug Discov. Today *11*, 481–493.

Shida, D., Kitayama, J., Yamaguchi, H., Okaji, Y., Tsuno, N.H., Watanabe, T., Takuwa, Y., and Nagawa, H. (2003). Lysophosphatidic acid (LPA) enhances the metastatic potential of human colon carcinoma DLD1 cells through LPA1. Cancer Res. *63*, 1706–1711.

Sinn, E., Muller, W., Pattengale, P., Tepler, I., Wallace, R., and Leder, P. (1987). Coexpression of MMTV/v-Ha-ras and MMTV/c-myc genes in transgenic mice: synergistic action of oncogenes in vivo. Cell *49*, 465–475.

Sotiriou, C., Wirapati, P., Loi, S., Harris, A., Fox, S., Smeds, J., Nordgren, H., Farmer, P., Praz, V., Haibe-Kains, B., et al. (2006). Gene expression profiling in breast cancer: understanding the molecular basis of histologic grade to improve prognosis. J. Natl. Cancer Inst. *98*, 262–272.

Taghavi, P., Verhoeven, E., Jacobs, J.J., Lambooij, J.P., Stortelers, C., Tanger, E., Moolenaar, W.H., and van Lohuizen, M. (2008). In vitro genetic screen identifies a cooperative role for LPA signaling and c-Myc in cell transformation. Oncogene *27*, 6806–6816.

Tibes, R., Qiu, Y., Lu, Y., Hennessy, B., Andreeff, M., Mills, G.B., and Kornblau, S.M. (2006). Reverse phase protein array: validation of a novel proteomic technology and utility for analysis of primary leukemia specimens and hematopoietic stem cells. Mol. Cancer Ther. *5*, 2512–2521.

Umezu-Goto, M., Kishimi, Y., Taira, A., Hama, K., Dohmae, N., Takio, K., Yamori, T., Mills, G.B., Inoue, K., Aoki, J., et al. (2002). Autotaxin has lysophospholipase D activity leading to tumor cell growth and motility by lysophosphatidic acid production. J. Cell Biol. *158*, 227–233.

Umezu-Goto, M., Tanyi, J., Lahad, J., Liu, S., Yu, S., Lapushin, R., Hasegawa, Y., Lu, Y., Trost, R., Bevers, T., et al. (2004). Lysophosphatidic acid production and action: validated targets in cancer? J. Cell. Biochem. *92*, 1115–1140.

Van Corven, E.J., Groenink, A., Jalink, K., Eichholtz, T., and Moolenaar, W.H. (1989). Lysophosphatidate-induced cell proliferation: identification and dissection of signaling pathways mediated by G proteins. Cell *59*, 45–54.

Van Meeteren, L.A., Ruurs, P., Stortelers, C., Bouwman, P., van Rooijen, M.A., Pradère, J.P., Pettit, T.R., Wakelam, M.J., Saulnier-Blache, J.S., Mummery, C.L., et al. (2006). Autotaxin, a secreted lysophospholipase D, is essential for blood vessel formation during development. Mol. Cell. Biol. *26*, 5015–5022.

Wegenka, U.M., Lütticken, C., Buschmann, J., Yuan, J., Lottspeich, F., Müller-Esterl, W., Schindler, C., Roeb, E., Heinrich, P.C., and Horn, F. (1994). The interleukin-6-activated acute-phase response factor is antigenically and functionally related to members of the signal transducer and activator of transcription (STAT) family. Mol. Cell. Biol. *14*, 3186–3196.

Xu, Y., Fang, X.J., Casey, G., and Mills, G.B. (1995). Lysophospholipids activate ovarian and breast cancer cells. Biochem. J. *309*, 933–940.

Yang, M., Zhong, W.W., Srivastava, N., Slavin, A., Yang, J., Hoey, T., and An, S. (2005). G protein-coupled lysophosphatidic acid receptors stimulate

proliferation of colon cancer cells through the β-catenin pathway. Proc. Natl. Acad. Sci. USA *102*, 6027–6032.

Yu, S., Murph, M.M., Lu, Y., Liu, S., Hall, H.S., Liu, J., Stephens, C., Fang, X., and Mills, G.B. (2008). Lysophosphatidic acid receptors determine tumorigenicity and aggressiveness of ovarian cancer cells. J. Natl. Cancer Inst. *100*, 1630–1642.

Zhang, X., Podsypanina, K., Huang, S., Mohsin, S.K., Chamness, G.C., Hatsell, S., Cowin, P., Schiff, R., and Li, Y. (2005). Estrogen receptor positivity in mammary tumors of Wnt-1 transgenic mice is influenced by collaborating oncogenic mutations. Oncogene *24*, 4220–4231.

Zhang, Q., Bhola, N.E., Lui, V.W., Siwak, D.R., Thomas, S.M., Gubish, C.T., Siegfried, J.M., Mills, G.B., Shin, D., and Grandis, J.R. (2007). Antitumor mechanisms of combined gastrin-releasing peptide receptor and epidermal growth factor receptor targeting in head and neck cancer. Mol. Cancer Ther. *6*, 1414–1424.